Steel wheels

- More than 90% of modem wheels are of pressed steel. They are strong and cheap to manufacture. They require negligible maintenance.
- Steel wheels are made from two pressings, as shown in cross section in figure.

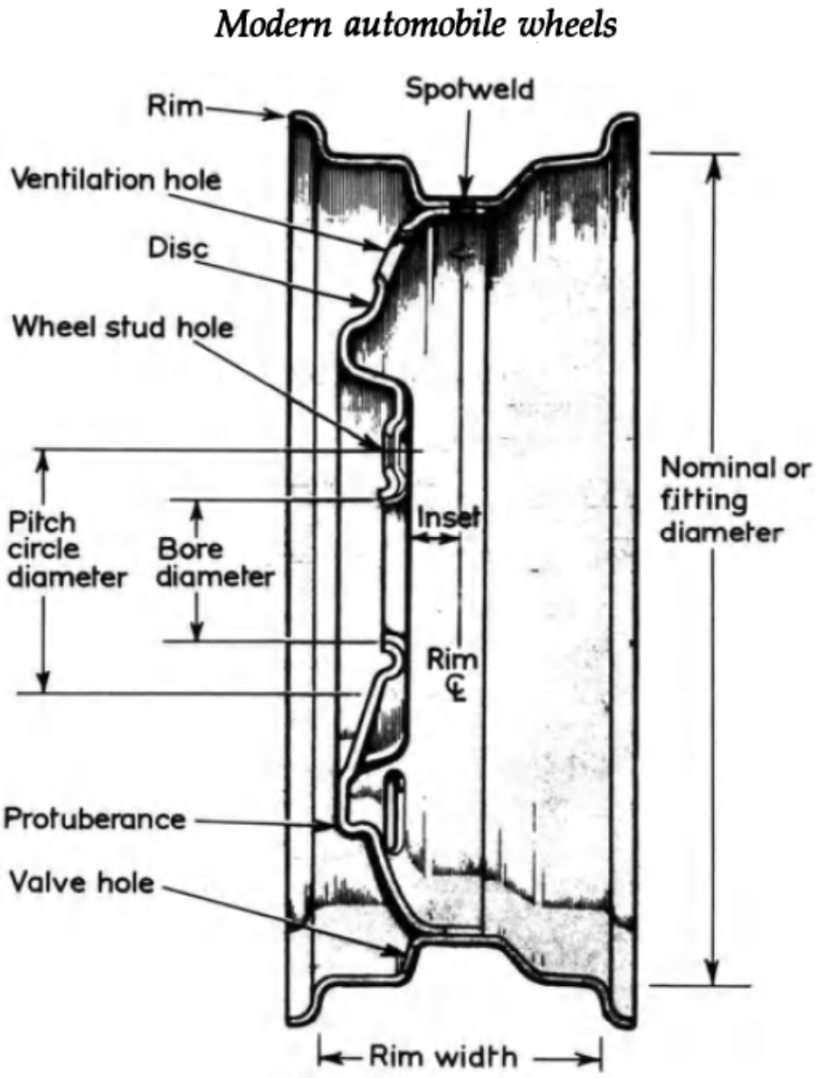

Aluminium alloy wheels

- Aluminium alloy wheels are usually made from heat-treated castings.
- The weight-saving compared, with a steel wheel varies from about 30-50% the saving being greater for the wider wheels.
- Specific heat-treatments are applied to improve appearance and to provide corrosion protection.
- Specific weight 2.7 g/cm3, G-AlSi10Cu

Magnesium alloy wheels

- A typical aluminium alloy has a density of about one-third that of steel. Cast magnesium alloys are even lighter, having a density of slightly less than one-quarter that of steel.
- The tensile strength is 40-50% of a typical steel pressing, giving a great improvement in the *specific strength* (tensile strength per unit density). Larger wheels yield a greater weight-saving.
- A 6JK x 15 steel wheel weights 10.3 kg. A magnesium replacement weights only 6.7 kg.
- **Magnesium alloy** produced exclusively for racing (specific weight 1,74 g/cm3, 35% lighter than aluminium alloy wheels. G-AlSi7Mg

Wire wheels

- The centre-lock wire wheel is traditionally associated with vintage sports cars and racing cars
- The weight-saving is negligible.

Invention of Pneumatic tyre

- Dunlop made his first pneumatic tyre in 1888.
- Robert William Thomson had patented a pneumatic tyre in 1845 (had even made measurements of the reduced tractive effort required to pull a light brougham over a paved road, a McAdam road and a surface of crushed granite, when a change was made from wrought-iron tyres to pneumatic ones.)

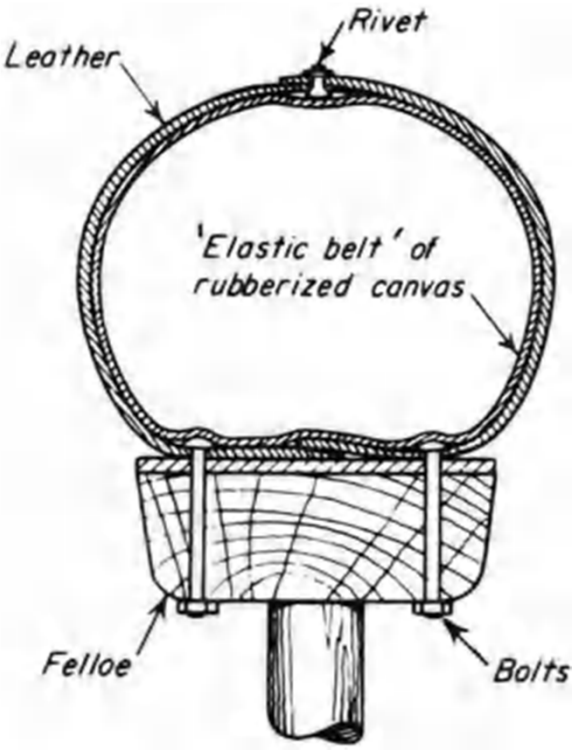

Thomson's original pneumatic tyre of 1845

Invention of Pneumatic tyre

- C. K. Welch, invented a *detachable* tyre incorporating high-tensile steel wires.

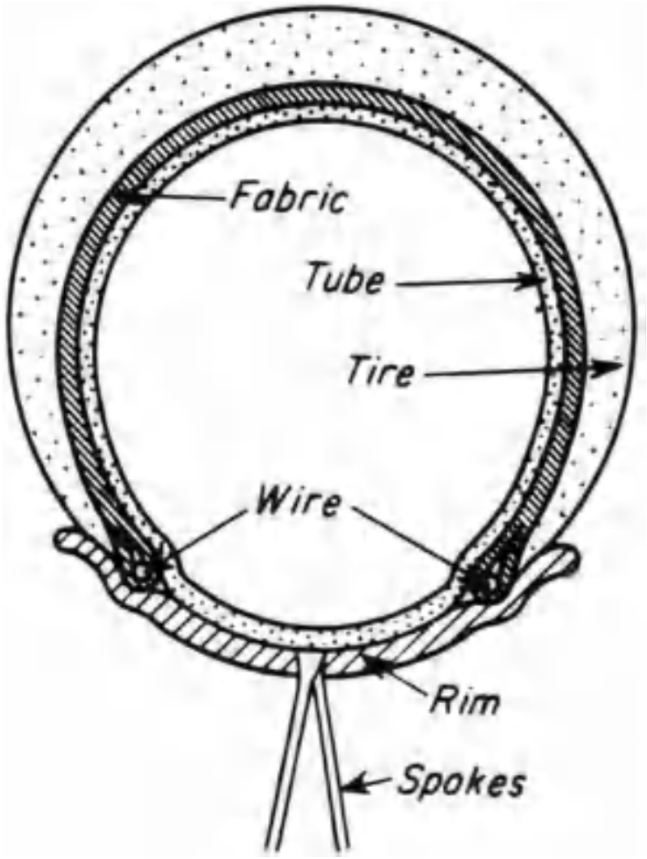

C. K. Welch's rim and bead design of 1890

Invention of Pneumatic tyre

- American, William Bartlett filed an invention with an improved beaded edge that was locked in position on the rim by the internal air pressure.
- Bartlett did not use steel wire in his beaded edge. By combining the two systems, (Barlett and Welch) we arrive at the beaded-edge construction used in 99% of modern tyres.

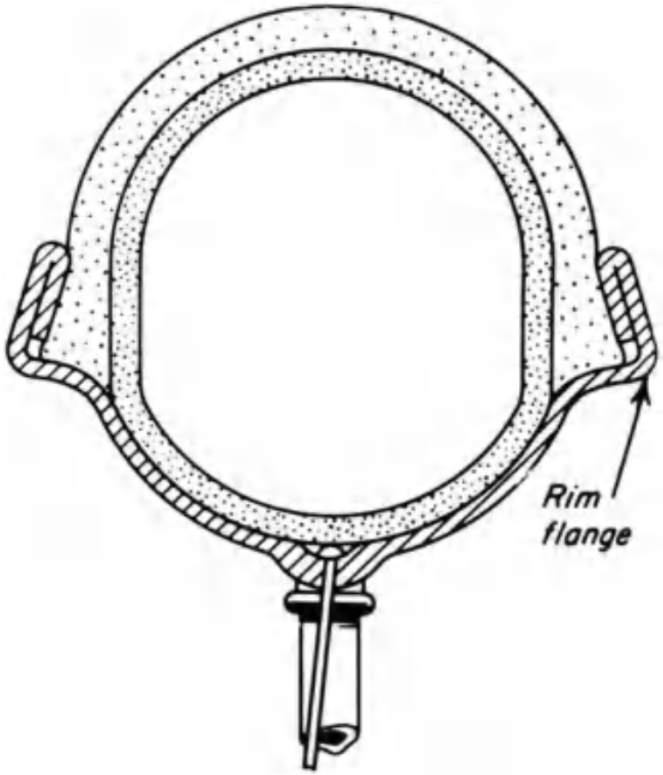

William Bartlett's rim and bead design of 1890.

Tyre construction

- Early tyre makers strengthen the walls of the tyre with a cotton - canvas reinforcement, By using both warp and weft interwoven in this manner, a chafing action resulted as the tyre section flexed at the road contact patch. This generated heat in the natural rubber compound and led to a rapid breakdown in the reinforcement. The average life of the early car tyre was about 2000 miles.

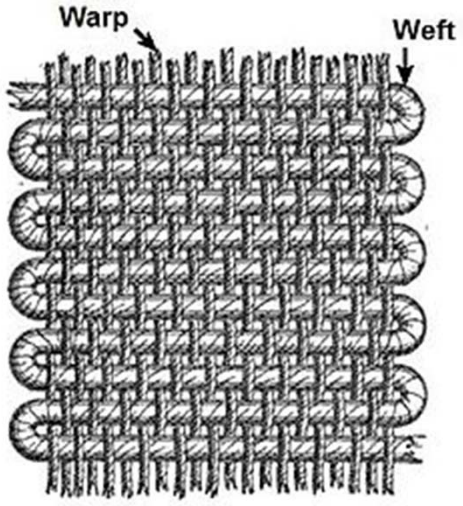

Tyre construction-Cross ply tires

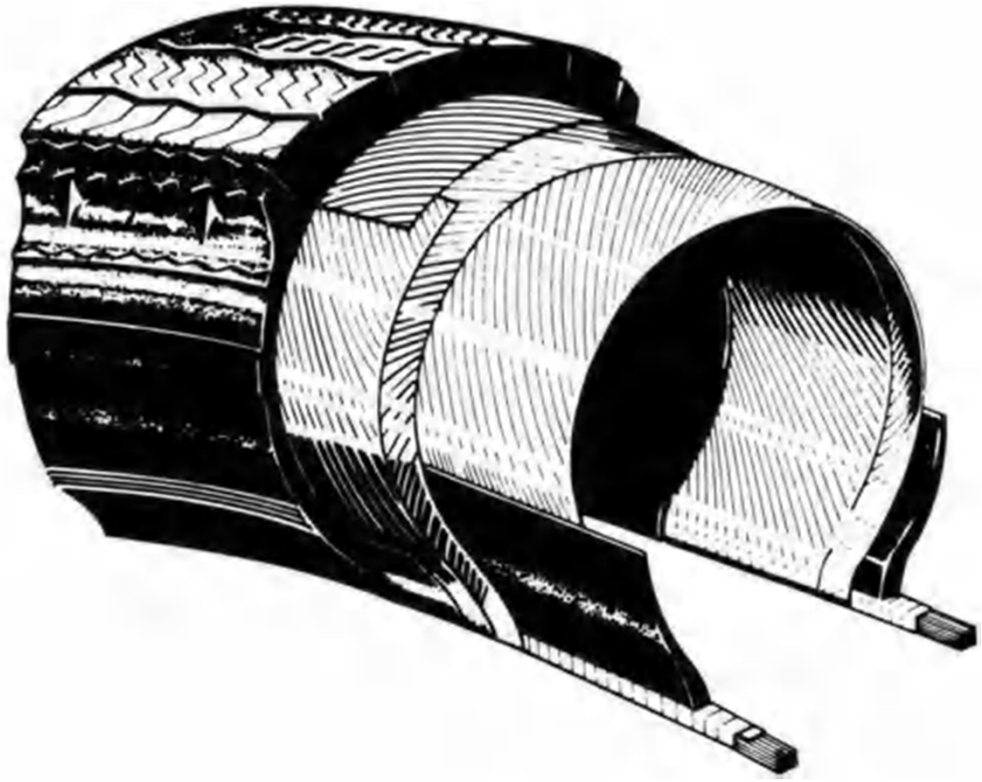

Internal construction of cross-ply tyre.

Tyre construction-Radial ply tires

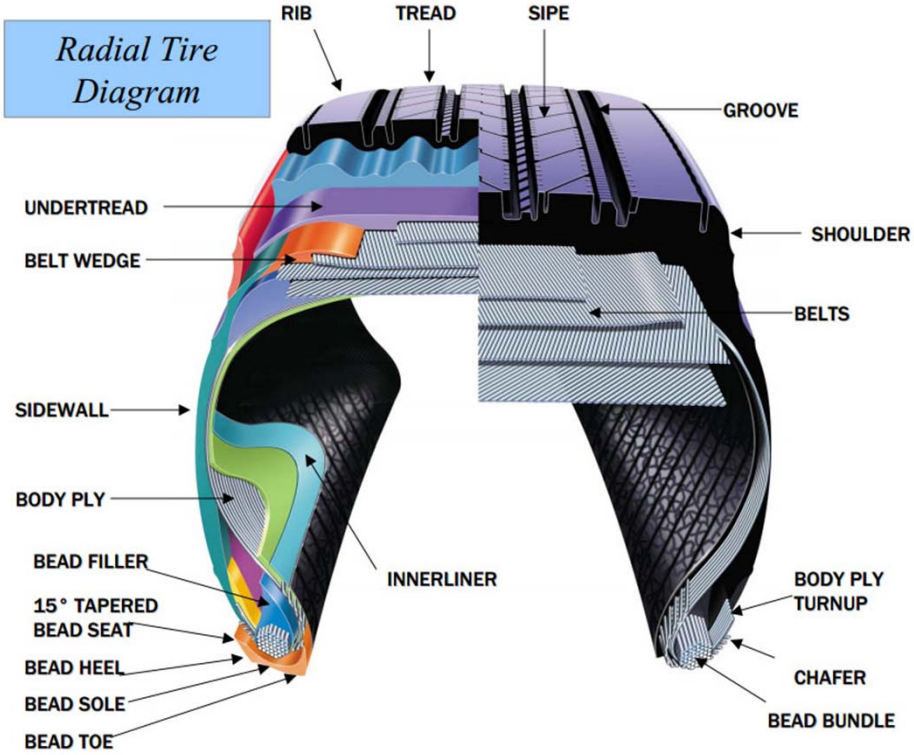

Internal construction of steel-braced radial tyre.

Michelin changed the method of tyre construction to reduce the amount of distortion in the footprint zone and immediately doubled the life of car tyres using identical compounds. Michelin stiffened the zone behind the tread by bands of steel mesh. They also increased the flexibility of the side walls by increasing the cord bias angle to 90°; hence the name 'radial', since the textile cords passed radially from inner to outer beaded edge.

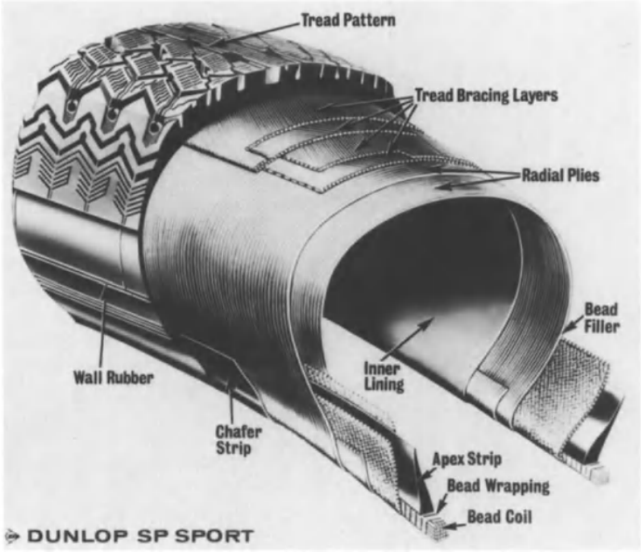

Tire Construction

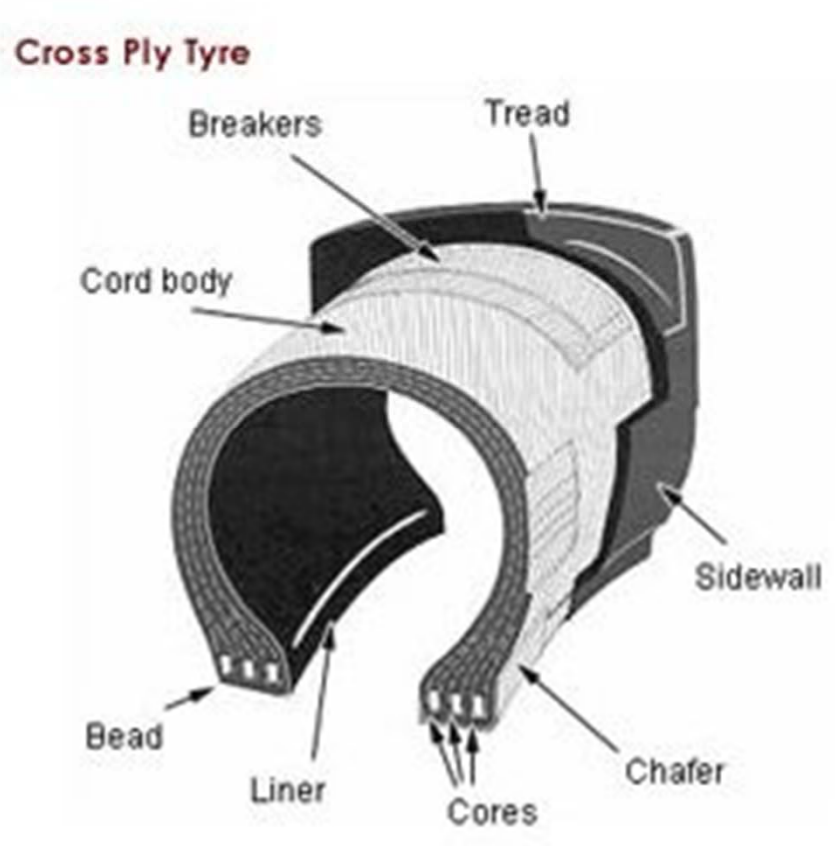

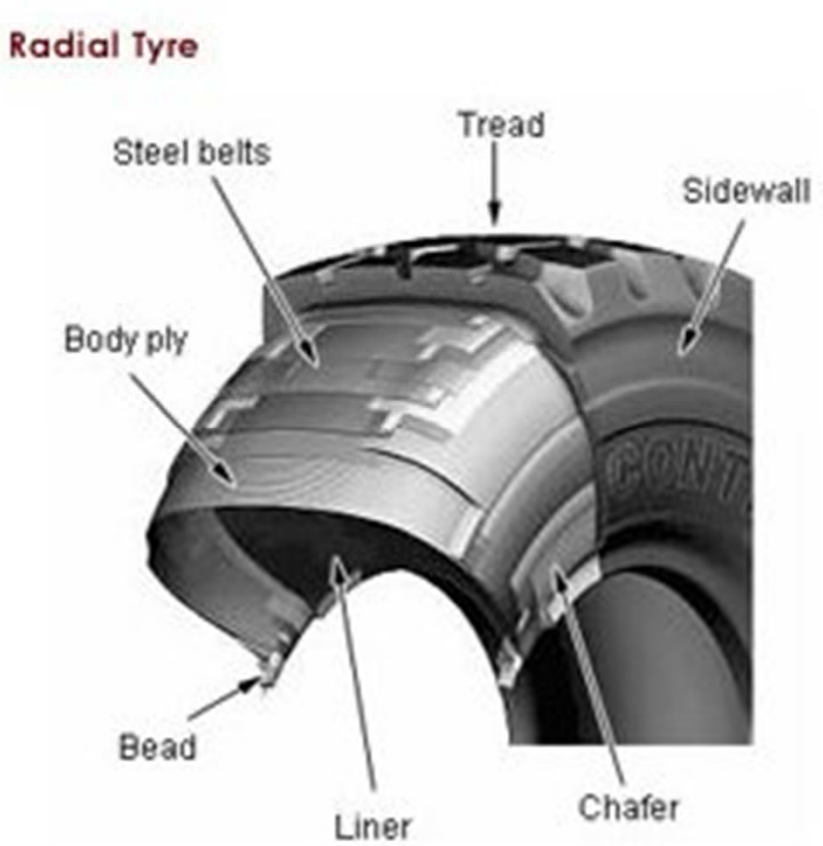

Materials used in a tyre

- The components of a modern radial tyre for passenger cars contain diverse ingredients in differing amounts. These ingredients vary by tyre size and tyre type (summer or winter tyre).
- The example below shows the ingredients used in the summer tyre 205/55 R 16 91V ContiPremiumContact 5 (The tyre shown here weighs about 8.5 kg without the rim).

Materials used in a tyre

Breakdown of ingredients

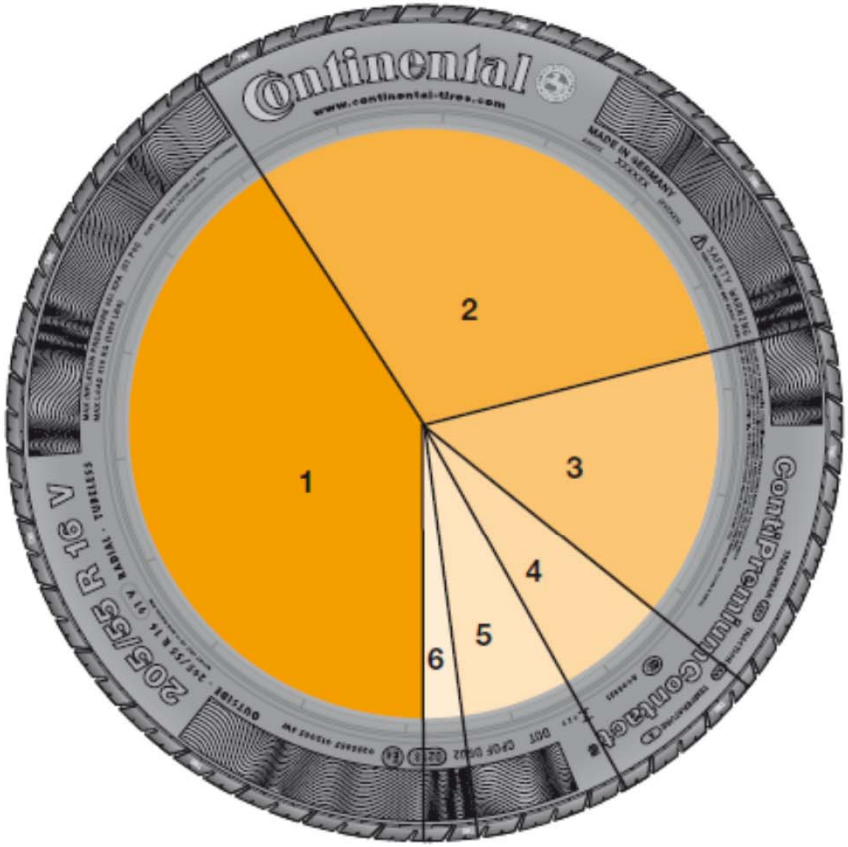

1 Rubber
(natural and synthetic rubber) 41%

2 Fillers
(carbon black, silica,
carbon, chalk ...) 30%

3 Reinforcing materials
(steel, polyester, rayon, nylon) 15%

4 Plasticizers (oils and resins)[1] 6%

5 Chemicals for vulcanisation
(sulphur, zinc oxide,
various other chemicals) 6%

6 Anti-ageing agents and
other chemicals 2%

Tyre Construction

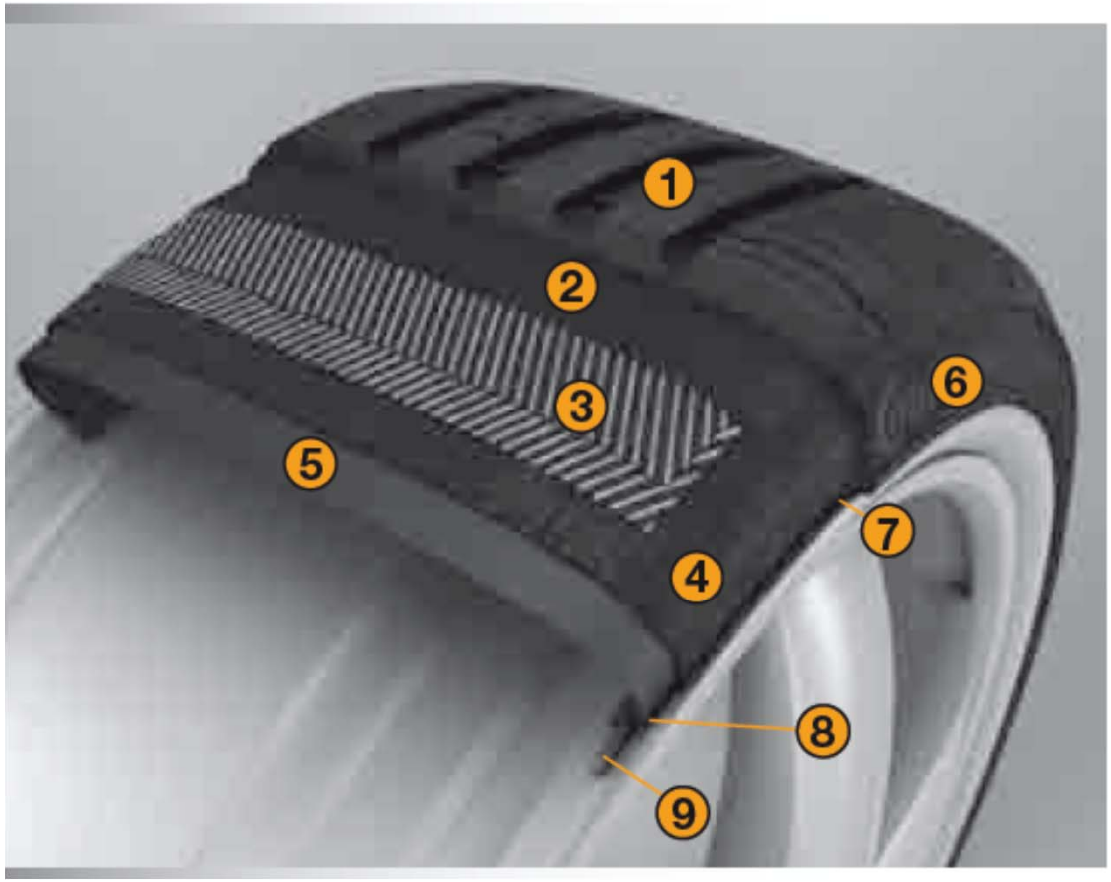

1. **Tread** – ensures high mileage, good road grip and water expulsion
2. **Jointless cap plies** – enable high speeds
3. **Steel-cord belt plies** – optimise directional stability and rolling resistance
4. **Textile cord ply** – controls internal pressure and maintains the tyre's shape
5. **Inner liner** – makes the tyre airtight
6. **Side wall** – protects from external damage
7. **Bead reinforcement** – promotes directional stability and precise steering response
8. **Bead apex** – promotes directional stability, steering performance and comfort level
9. **Bead core** – ensures firm seating on the rim

Tyre Construction-Tread/Belt Assembly

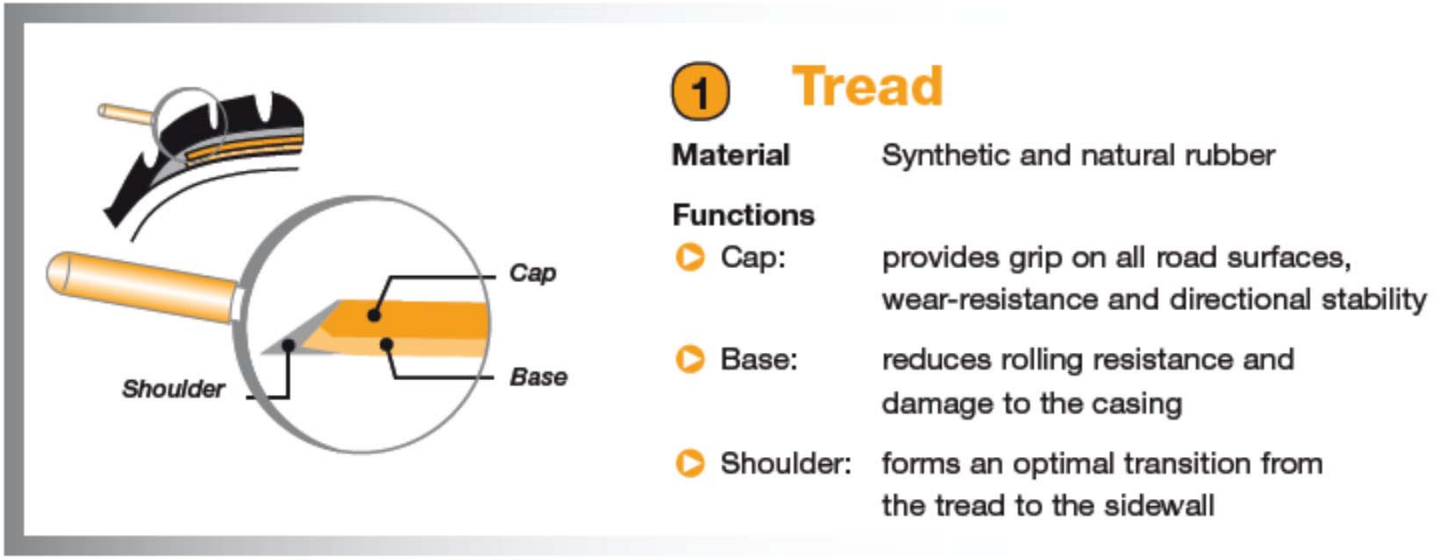

Tyre Construction-Tread/Belt Assembly

Tyre Construction-Tread/Belt Assembly

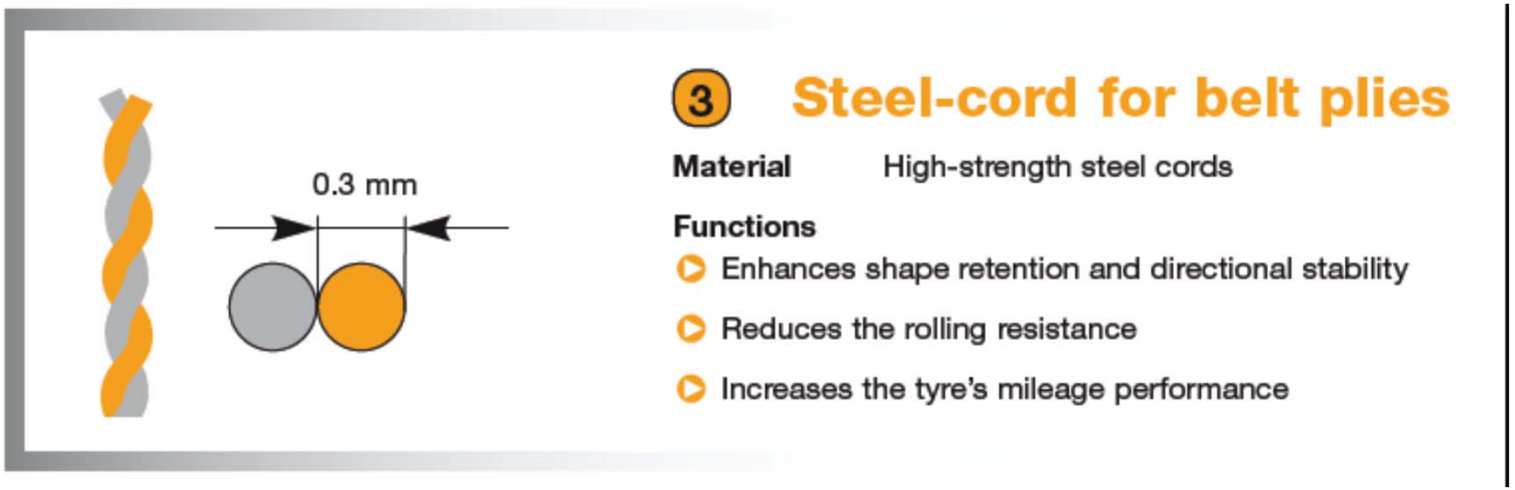

Tyre Construction-Carcass

4 Textile cord ply

Material Rayon or polyester (rubberised)

Function

- Controls internal pressure and maintains the tyre's shape

Tyre Construction-Carcass

5 Inner liner

Material Butyl rubber

Functions

- Seals the air-filled inner chamber
- Acts as a tube in tubeless tyres

Tyre Construction-Carcass

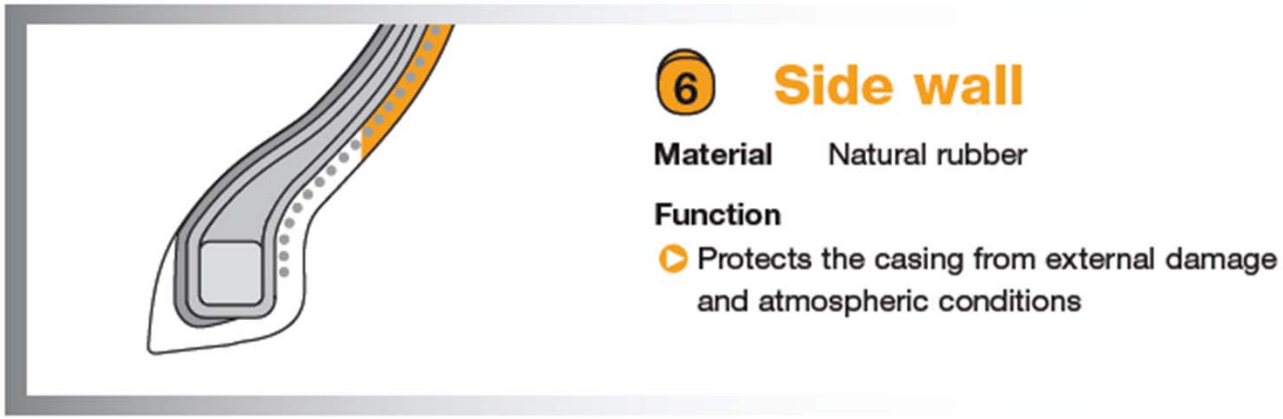

6 Side wall

Material Natural rubber

Function

- Protects the casing from external damage and atmospheric conditions

Tyre Construction-Carcass

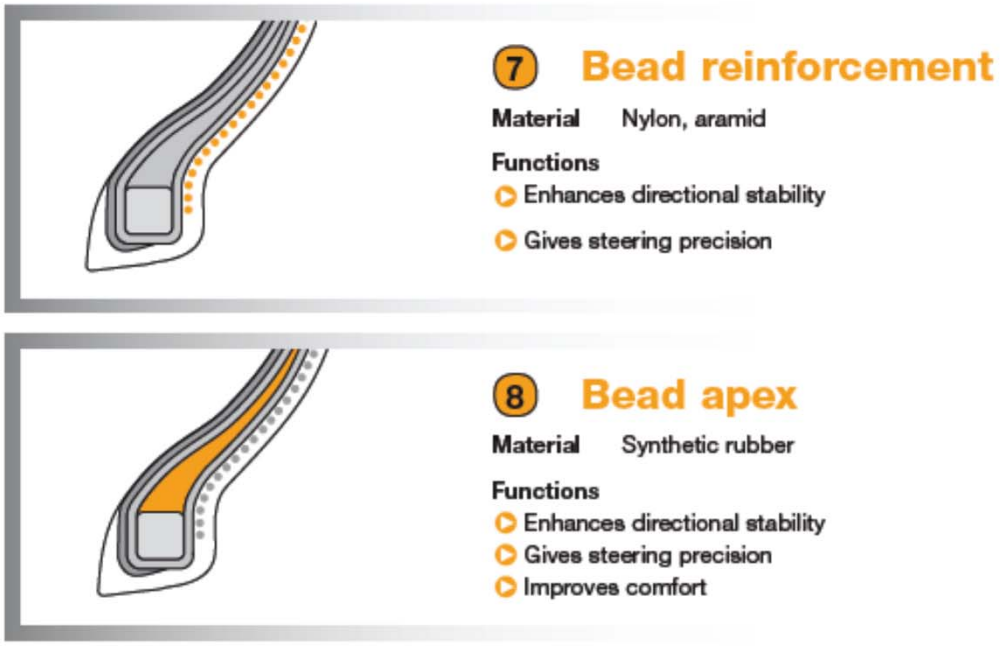

7 Bead reinforcement

Material Nylon, aramid

Functions

- Enhances directional stability
- Gives steering precision

8 Bead apex

Material Synthetic rubber

Functions

- Enhances directional stability
- Gives steering precision
- Improves comfort

Tyre Construction-Carcass

9 Bead core

Material Steel wire embedded in rubber

Function

- Ensures that the tyre sits firmly on the rim

Tyre testing

- American Society for Testing Materials standardized a Standard Pavement Skid Test Tire in their specification ASTM-E17.
- The type and condition of the road surface is just as important as the tyre. On wet road surfaces the coefficient of friction could vary from almost zero to 0.7. On dry roads the variation was less drastic, being from 0.4 to 0.87.

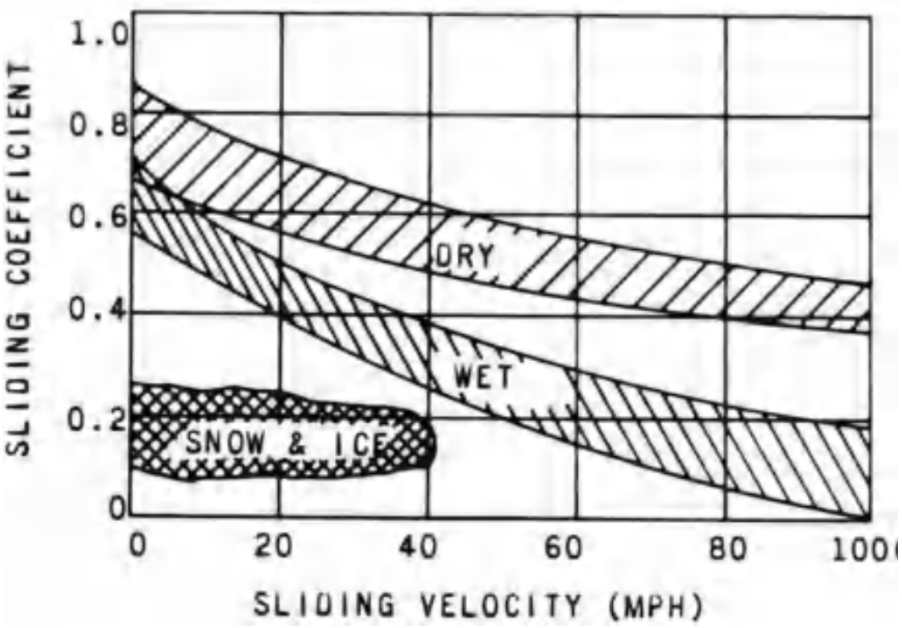

Cornering force-sideslip curve

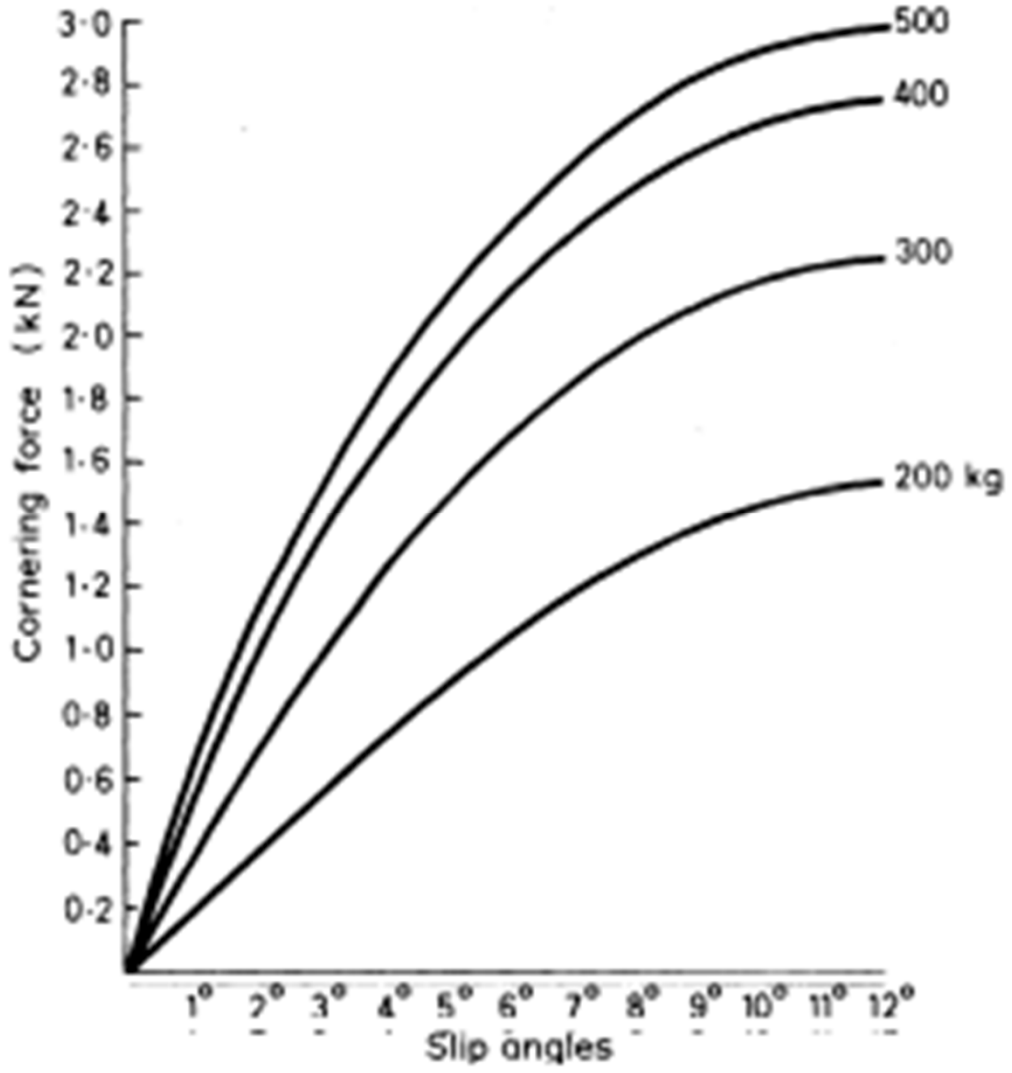

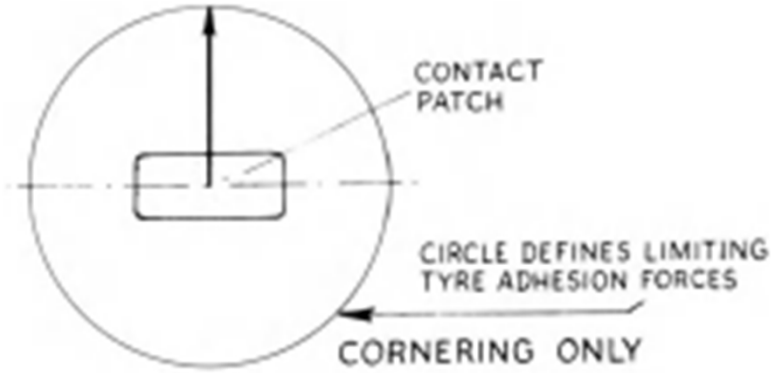
CONTACT
PATCH
CIRCLE DEFINES LIMITING
TYRE ADHESION FORCES
CORNERING ONLY

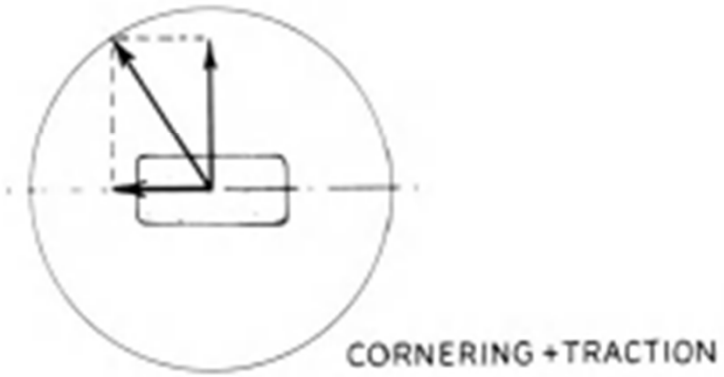
CORNERING + TRACTION

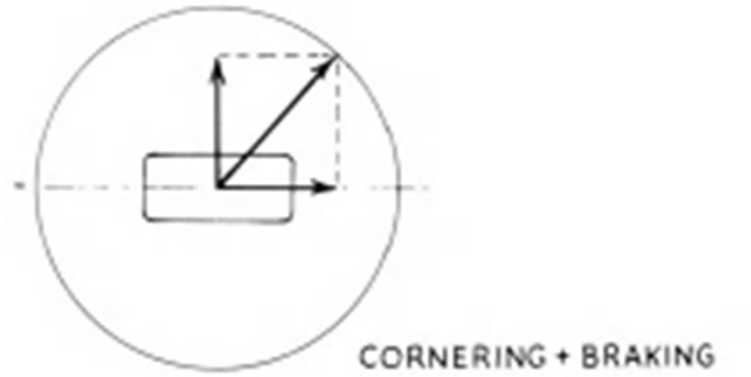
CORNERING + BRAKING

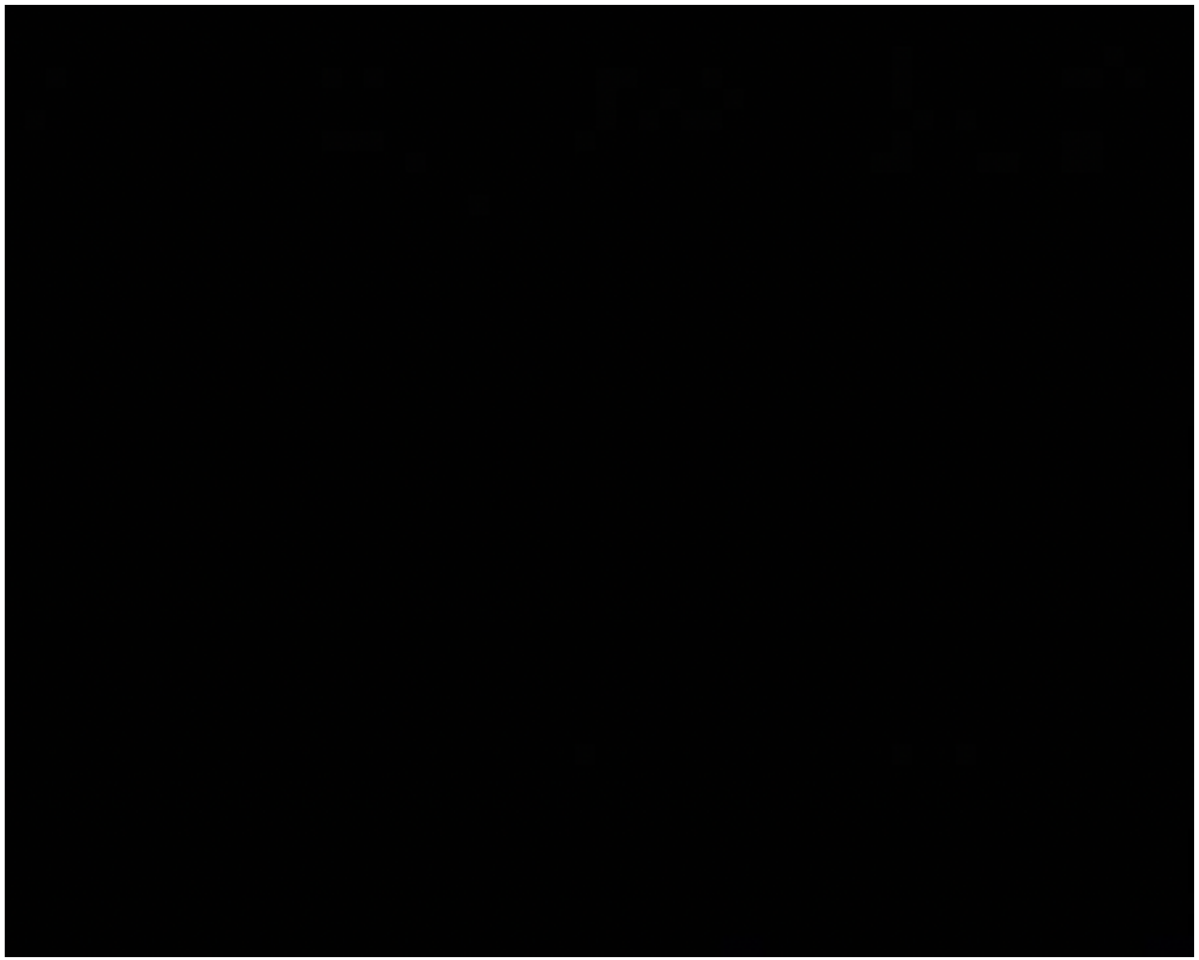

Hydroplanning

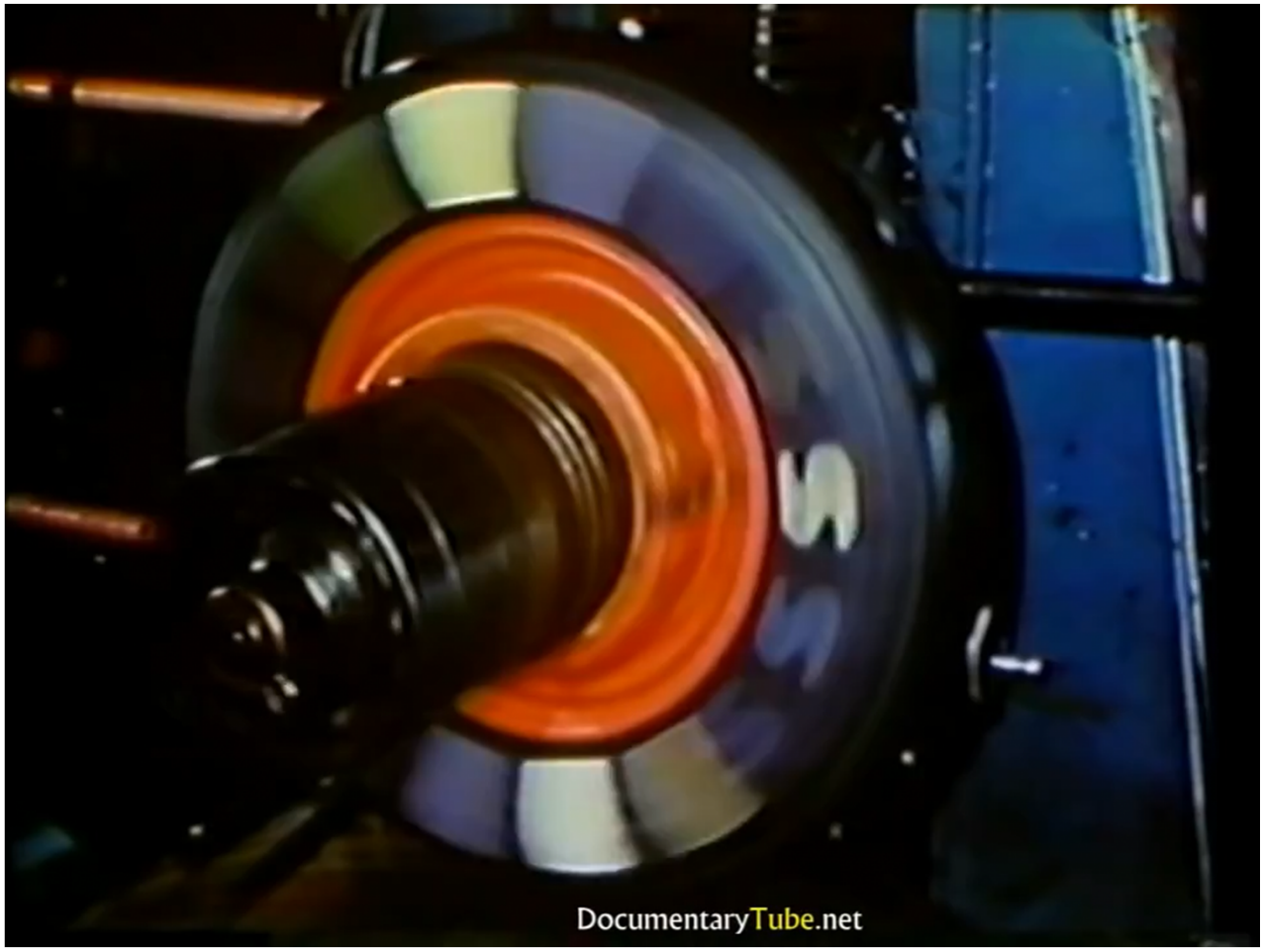

- The tire is the most critical component for vehicle dynamic behavior in the longitudinal, lateral, and vertical directions. With the exception of inertial and aerodynamic forces, all forces and moments acting on the vehicle are applied at the contact patch between the tire and the road surface. The friction of the tire against the roadway enables forces to be transferred at the contact patch.
- The amount of force which can be transferred is dependent on the frictional properties of both the tire and the roadway. The transfer of force between tire and roadway is made possible by two main forms of friction:

✓ adhesive friction (intermolecular adhesion)

✓ hysteretic friction (interlocking forces). A tire's hysteretic friction against the road surface is dependent on the amount of contact between the tire's tread blocks and the roughness on the road surface.

A tire made from a material with a large damping coefficient will also have a high coefficient of friction due to increased hysteretic friction. Tire adhesive friction takes place on the molecular level (on the order of 10e-5 mm) and requires a direct contact between the roadway and the tire's tread surface. On a dry roadway, adhesive friction makes up the majority of tire friction. Figure shows a visual depiction of the difference between adhesive friction and hysteretic friction in a tire's contact patch.

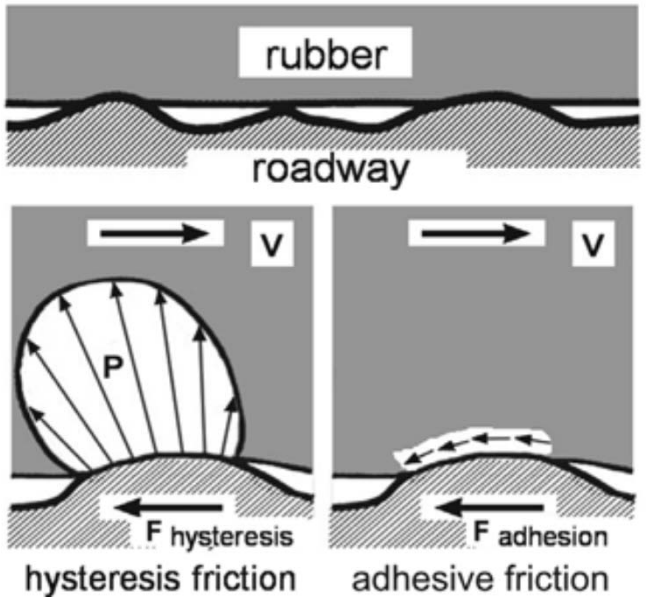

*Chassis Handbook, M. ERSOY, B. Heissing

- The influence of a tire's hysteretic friction component on a wet roadway can be increased by optimizing the tire's drainage properties and tread pattern.
- If a tire's tread pattern can effectively drain the water from the contact patch, the molecular forces between tire and roadway can be restored. While driving on snow and ice at very low ambient temperatures, a tire's adhesive friction is responsible for the entire frictional force between tire and road surface. This is due to the fact that at very low temperatures, a tire's rubber compound reaches its glass transition temperature and is no longer viscoelastic enough to wrap itself around roadway irregularities to provide traction.

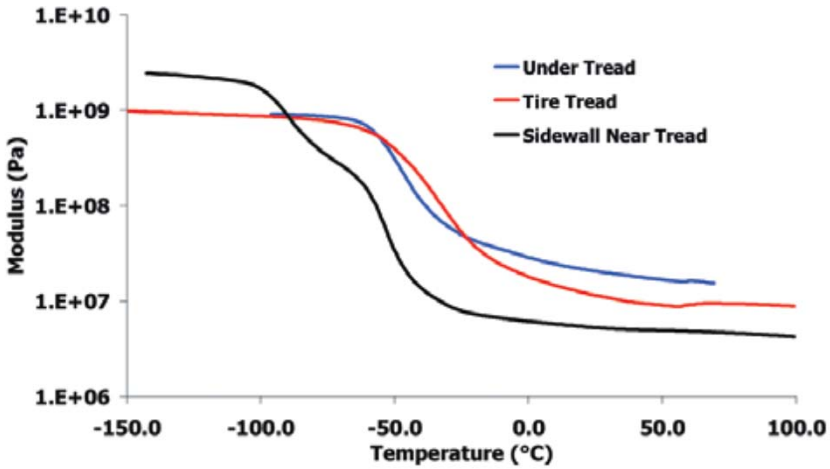

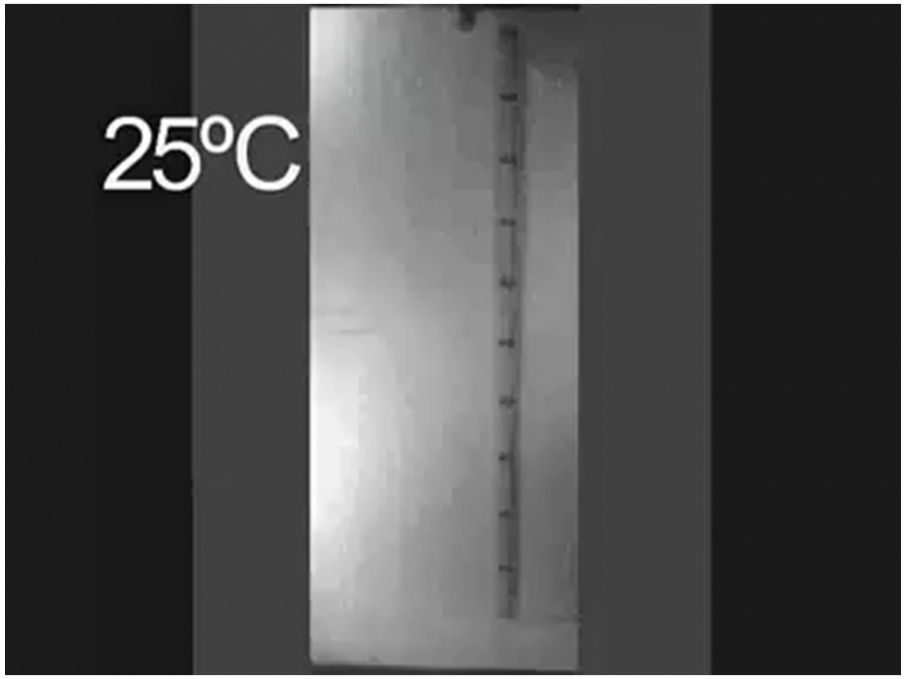

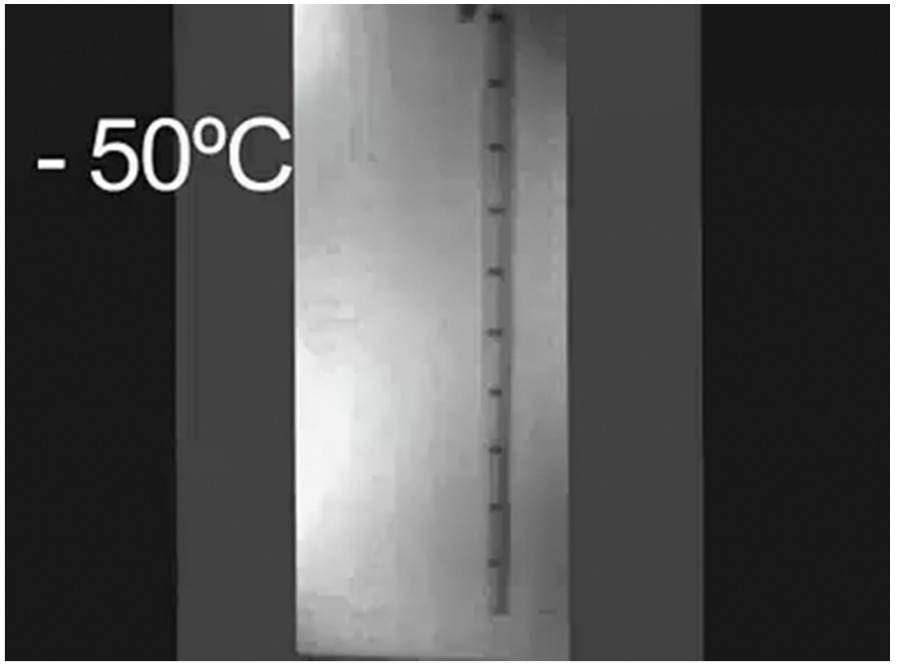

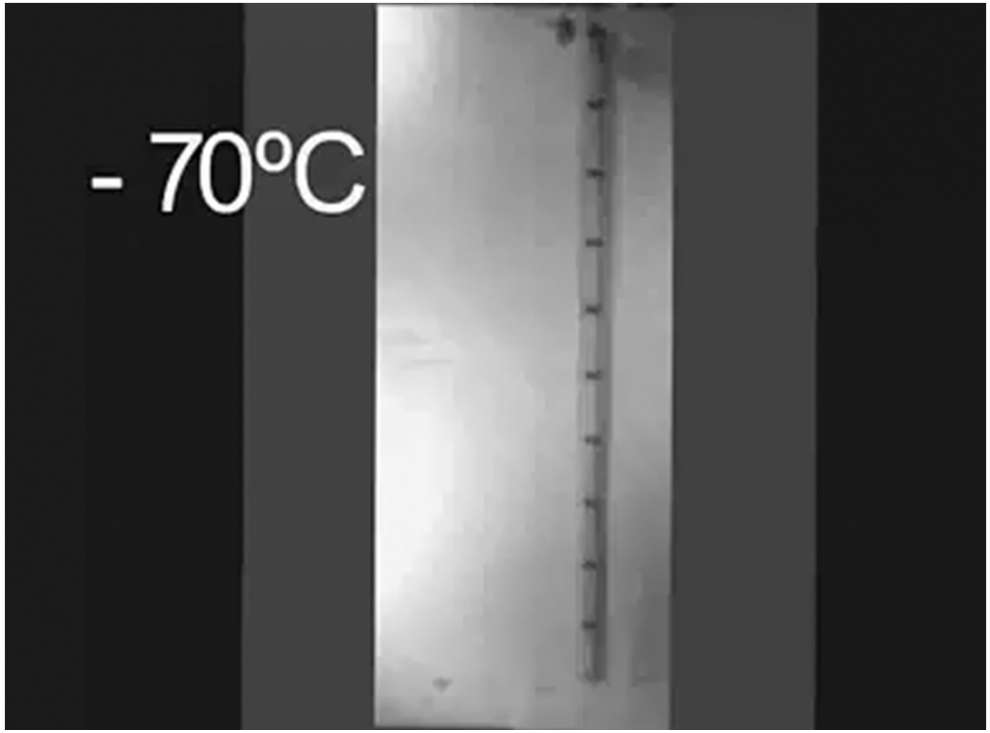

https://www.doitpoms.ac.uk/tlplib/glass-transition/demos.php

- The transition from “sticking” to “slipping” is determined by the relative speed between the tire tread and the road surface. To achieve the largest possible frictional coefficient μ, surface pressure should be evenly distributed and relative speed kept as low as possible. In order to optimize traction, a tire’s rubber compound must be exactly matched to the standard temperatures, pressure loads, velocities, and excitation frequencies that occur during normal driving conditions. The transfer of force in the contact patch of a rolling tire is always combined with an elastic deformation of the tread profile and a structural tire deformation.

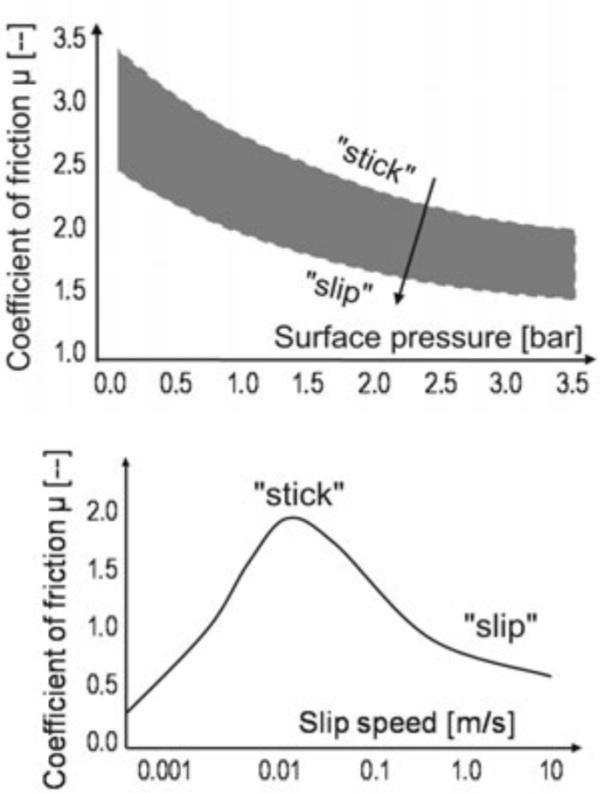

*Chassis Handbook, M. ERSOY, B. Heissing

- While driving, a tire is subjected to four types of loading. These different load types typically act simultaneously. The four load types are:

✓ free rolling

✓ vertical force transfer

✓ braking / acceleration

✓ cornering (tire slip / camber)

*Chassis Handbook, M. ERSOY, B. Heissing

- I: Load capacity of the (deflated) tire's structure,
- II: Air pressure force acting on the tire walls to maintain the tire's round shape,
- III: Force resulting from the compression of the air within the tire,
- IV: Load capacity of the air in the tire

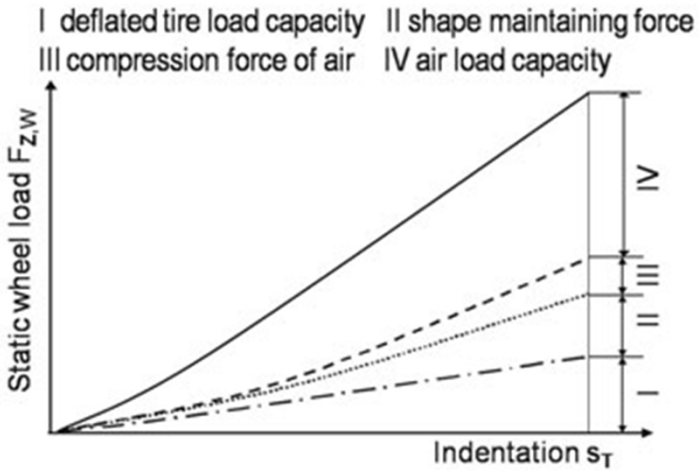

*Chassis Handbook, M. ERSOY, B. Heissing

- The contact patch area (AT) describes the entire road surface area within the edges of the contact patch. The actual contact patch area (AT_real) depends on the fraction of the tire's tread profile that is actually in contact with the road surface, and can be much smaller than AT. The fraction is usually between 60% and 80%. As a result, the local pressure on the tread blocks in the actual contact patch can be higher than the tire's fill pressure. The average pressure in the actual contact patch can be 1 to 2 bar greater than the tire pressure. The roughness of the road surface can also cause the local pressure in the contact patch to be higher than the tire inflation pressure.
- Road surface roughness can reduce the actual contact patch area to between 7% and 60% of the AT_real. This further reduction can result in pressure peaks of up to 45 bar for passenger vehicle tires

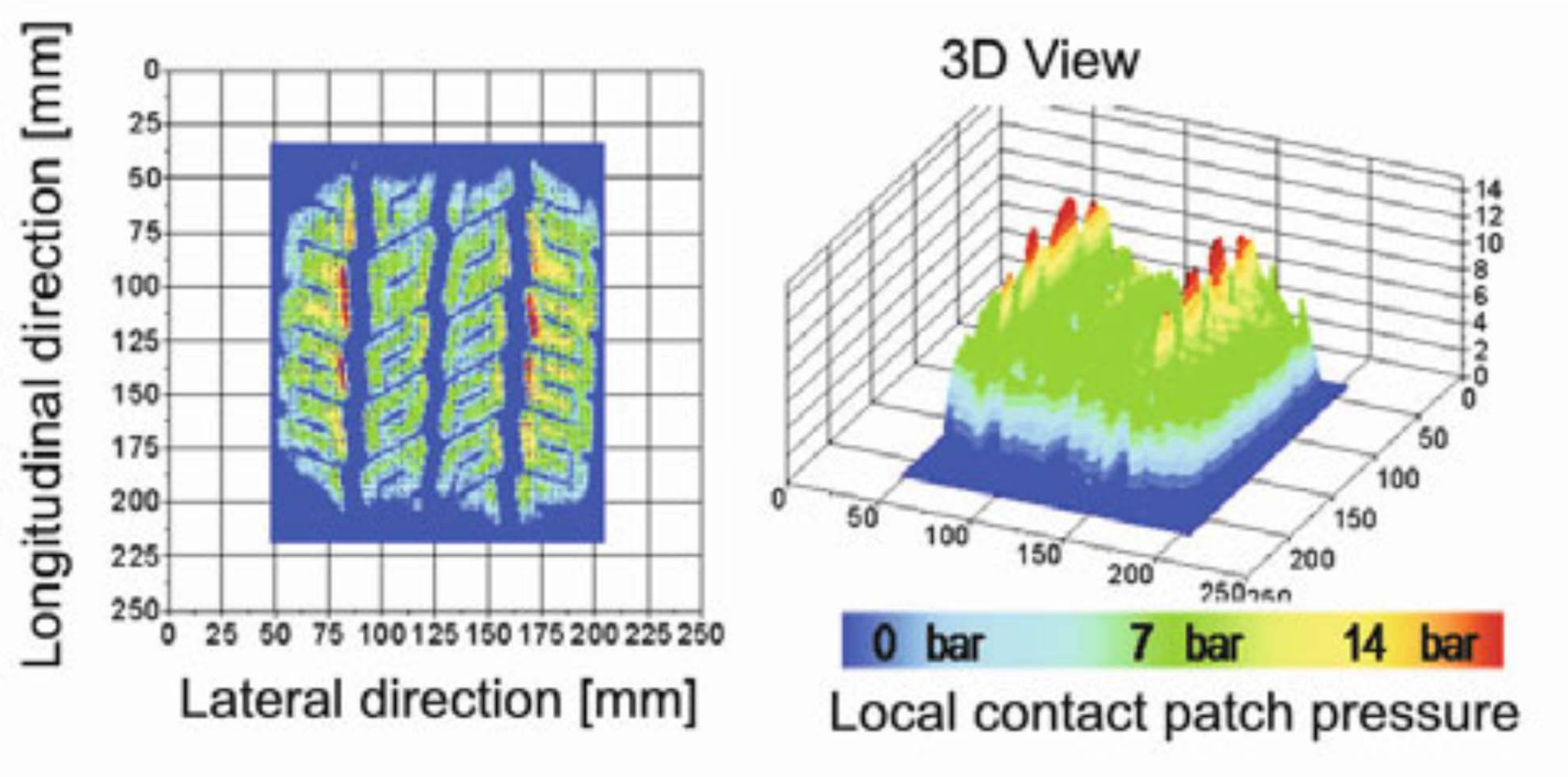

*Chassis Handbook, M. ERSOY, B. Heissing

- The influence of the tire's inflation pressure pT on the vertical spring rate of a passenger vehicle tire can be seen qualitatively in Figure.
- The figure show that the spring rates are linear in the tire's operating range. In the tire's operating range, the relationship between the vertical wheel load FZ_W and the vertical tire deformation sT is nearly linear. As a result, the tire stiffness cT can be assumed to be constant.

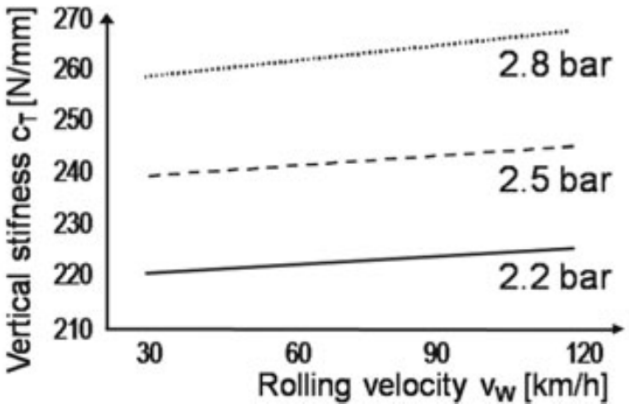

*Chassis Handbook, M. ERSOY, B. Heissing

- The transfer of a horizontal force FX_W or FY_W through the tire's contact patch area AT is always accompanied by a certain amount of slip between tire and roadway.
- This is due to the elasticity of the tire's tread profile and structure as well as the momentary coefficient of friction between tire and roadway. The slip between tire and roadway is made up of two components: deformation (deformation of the tire's tread blocks) and relative movement (relative movement between the tire and the roadway).

*Chassis Handbook, M. ERSOY, B. Heissing

Figure shows the distribution of shear stress resulting from tread block deformation in the contact patch of a tire being acted on by a braking force FX_W. The condition depicted includes partial tire slip, whereby the tire's force threshold is defined by a maximum shear force. If the local surface pressure and the local coefficient of static friction combine to exceed this maximum shear force, the tire's behavior is determined by the coefficient of sliding friction.

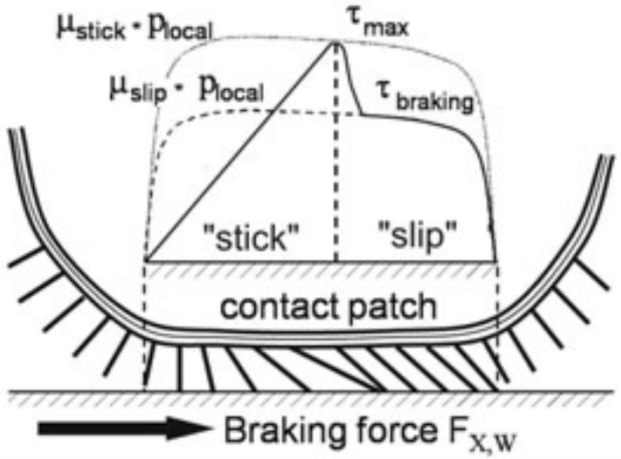

*Chassis Handbook, M. ERSOY, B. Heissing

The total tire slip is a combination of the tire's deformation and its movement relative to the roadway. In practice, most vehicle dynamic analyses do not differentiate between the two types of tire slip (deformation and relative motion). Most analyses define one global tire slip for the longitudinal direction, and one for the lateral direction. The maximum coefficient of friction between the tire and the roadway is reached during partial sliding, at a slip value of approximately 10% - 30%.

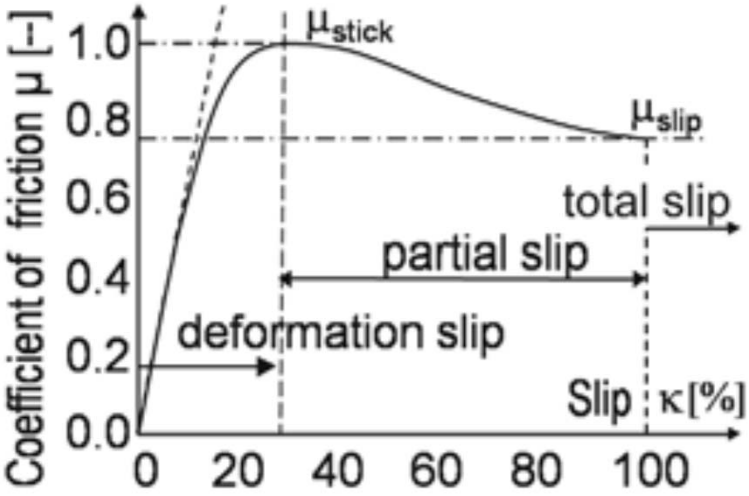

*Chassis Handbook, M. ERSOY, B. Heissing

A tire does not have a single coefficient of static friction or a single coefficient of sliding friction. Instead, a continuous curve can be plotted for the tire's frictional behavior. This curve depicts the tire's longitudinal coefficient of friction μ as a function of wheel vertical load FZ_W, tire pressure, driving speed ,slip and th condition of the road surface.

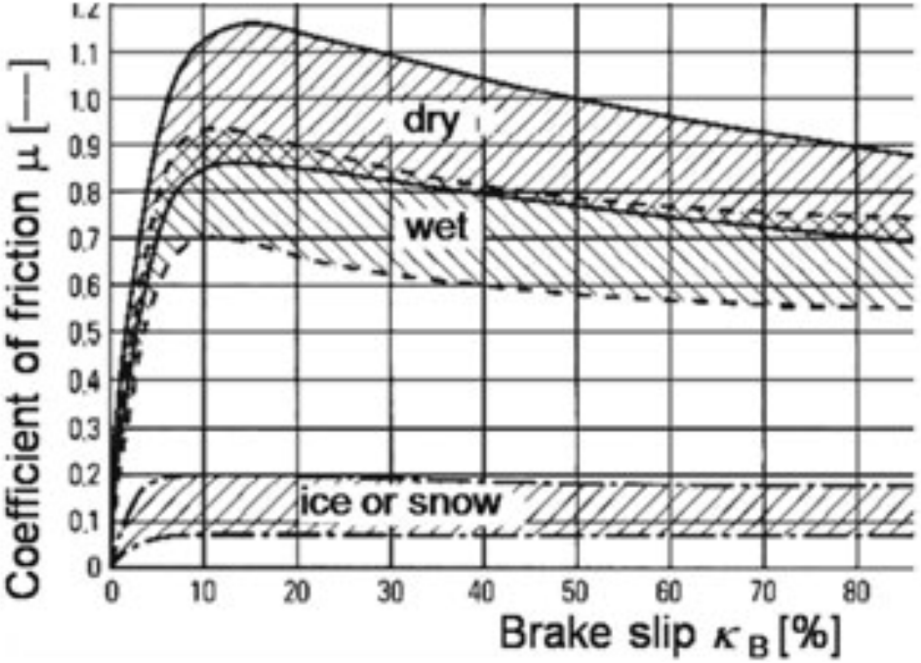

Road surface type	*Friction Coefficient μ*
Sod, turf (damp)	0.55 – 0.25
Loam (wet/dry)	0.45 – 0.50
Loam / clay (wet/dry)	0.55 – 0.30
Topsoil (wet/dry)	0.40 – 0.30
gravel (hard packed/loose)	0.35 – 0.30
sand (hard packed/loose)	0.30 – 0.35

*Chassis Handbook, M. ERSOY, B. Heissing

The curves in Figure illustrate the effect of vehicle speed on the frictional coefficient. Higher speeds cause increased relative velocity in the sliding part of the contact patch. This leads to a lower coefficient of sliding friction.

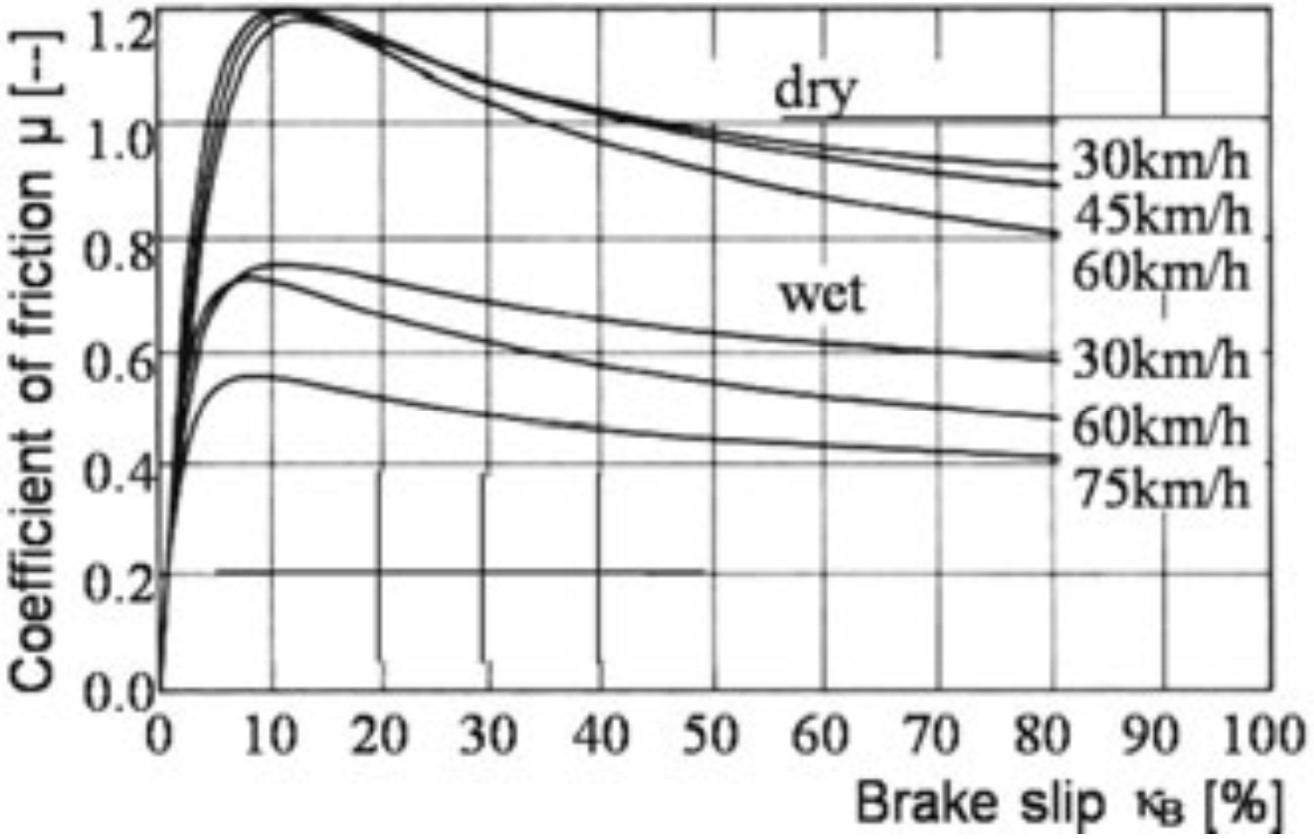

*Chassis Handbook, M. ERSOY, B. Heissing

A typical curve mapping for brake force FX_W versus braking slip under various vertical wheel loads FZ_W can be seen in Figure. The curves in Figure were experimentally determined using a rolling drum type test stand. As an initial approximation, it can be assumed that brake force and acceleration force characteristics are symmetric with one another. This is especially true for tires with direction-independent tread patterns.

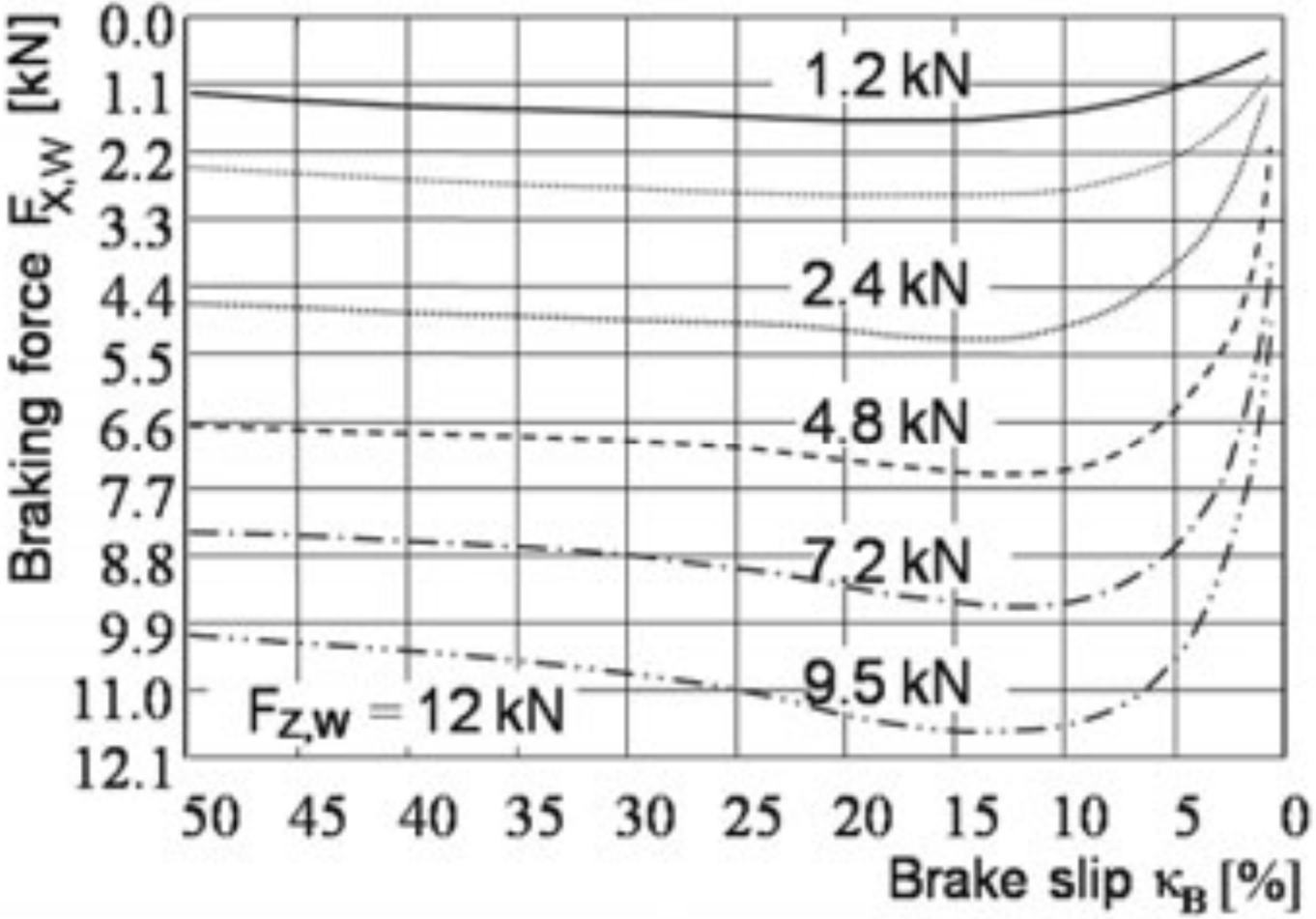

*Chassis Handbook, M. ERSOY, B. Heissing

The method by which lateral forces FY_W are transferred through the tire's contact patch area AT is similar to that of longitudinal forces. As a result of lateral elasticities in the tire's tread and structure, force transfer can only occur when the tire is elastically deformed. This lateral deformation is directly linked with lateral tire slip S. The tire's lateral slip is characterized by a sideslip angle α. When a lateral force FY_W is acting on the tire, the sideslip angle α is the angle between the tire's actual direction of travel and its rolling direction.

$$S_\alpha = \frac{v_{W,lateral}}{v_{W,long}} = \frac{v_W \cdot \sin(\alpha)}{v_W \cdot \cos(\alpha)} = \tan(\alpha)$$

*Chassis Handbook, M. ERSOY, B. Heissing

As a tread block enters the contact patch area AT, it is pressed against the road surface. The local pressure and the coefficient of static friction cause the block to follow the wheel's direction vector vW kinematically. As the tread block moves through the contact patch, the sideslip angle α between the tire's direction vector vW and its midplane cause the tread block to be deflected relative to the tire's circumference, to which it is attached. This elastic deflection causes a shear force τ within the tread block's rubber. This deflection also causes the tread block to slip. As the tread block moves through the contact patch, the kinematic deflection increases, as does the shear stress τ in the rubber. The tread block is supported at one end by its attachment to the tire's circumference, and at the other end by its frictional coefficient μ against the road surface. The tread block's traction against the road surface can only transfer a force that is lower than the maximum shear stress τ_max at the adhesion limit. The adhesion limit is determined by the coefficient of friction μ and the local pressure plocal. Once the shear stress in the tread block reaches the maximum shear τ_max, the tread block's surface loses grip and begins to slide.

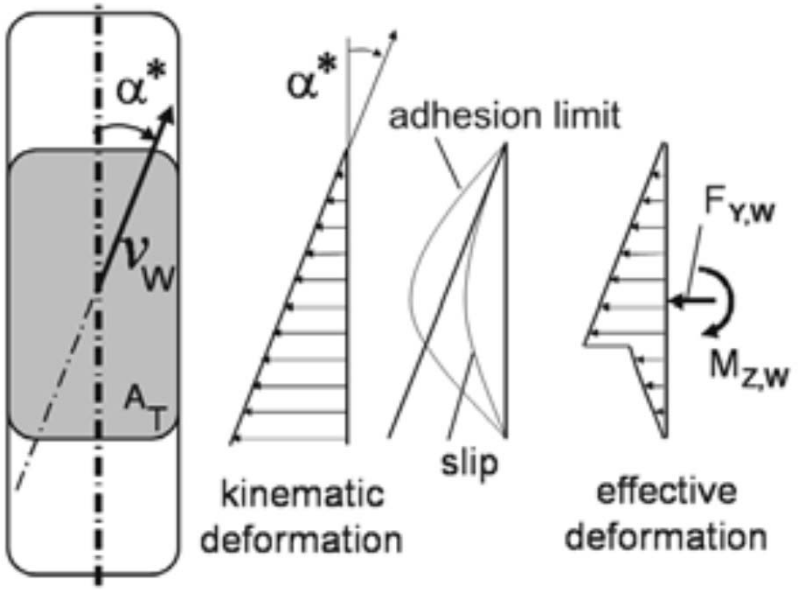

$$F_{\mathrm{Y,W}} = \int_{A_\mathrm{T}} \tau_\alpha(A) \cdot \mathrm{d}A$$

*Chassis Handbook, M. ERSOY, B. Heissing

For very small sideslip angles (α<2°to3°), the shear stress distribution τ takes the form of a triangle. This is because the maximum shear stress has not yet been reached and the entire lateral slip is due to tread block deflection. In such a case, the relationship between the lateral force FY_W and the sideslip angle α is linear. As the sideslip angle increases, the proportion of the total lateral tire slip made up by sliding (rather than by deformation) increases. Under these circumstances, the shear stress distribution is no longer purely triangular. The non-triangular portion of the shear stress distribution represents the shear force distribution in the slipping portion of the contact patch. For larger sideslip angles, the lateral force FY_W curve relative to the sideslip angle exhibits a decreasing slope. This curve eventually flattens to a constant as the tire slides across the road surface.

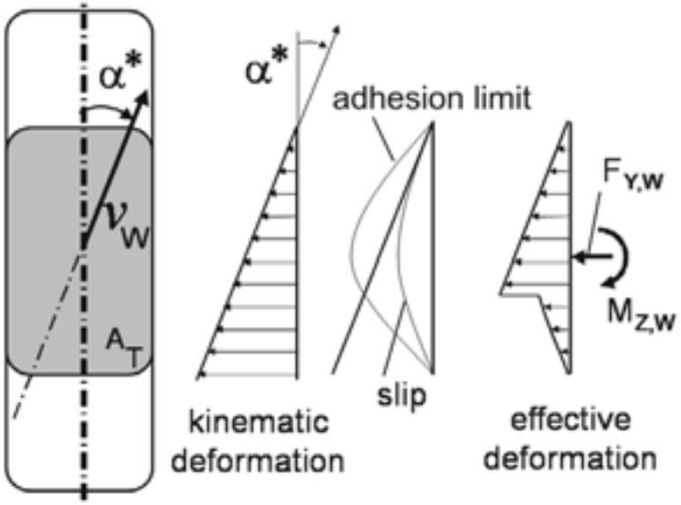

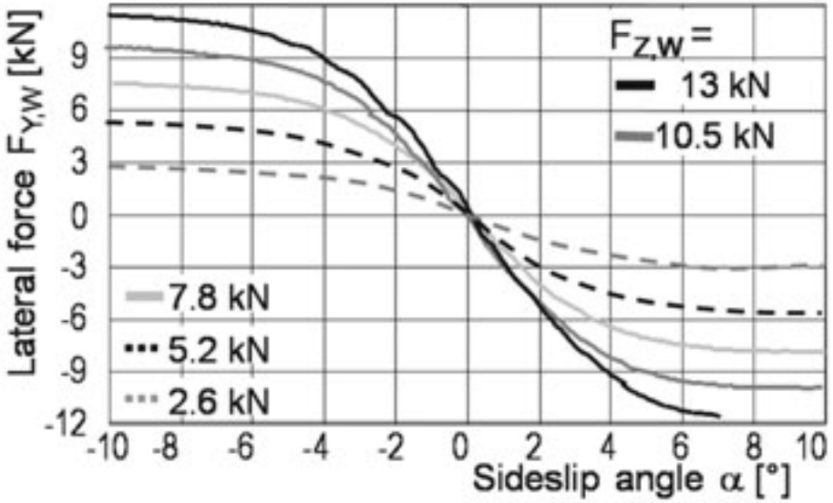

*Chassis Handbook, M. ERSOY, B. Heissing

On dry road surfaces, the relationship between the lateral force FY_W and the sideslip angle α is nearly linear for values of |α| < 3°. This range of sideslip angles corresponds to a vehicle lateral acceleration of up to 0.4 g. In this linear region, the tire's lateral force FY_W as a function of the sideslip angle α can be calculated using the (vertical load dependent) tire stiffness constant c:

$$c_\alpha = \left.\frac{\mathrm{d}\left(F_{\mathrm{Y,W}}\right)}{\mathrm{d}\alpha}\right|_{\alpha=0^\circ}$$

$$F_{\mathrm{Y,W}} = c_\alpha \cdot \alpha \quad \text{for} \quad |\alpha| < 3^\circ$$

*Chassis Handbook, M. ERSOY, B. Heissing

The tire's shear stress distribution in its contact patch is not symmetric about the tire's rotational (or "lateral") axis. Therefore, every lateral force FY_W which occurs in the tire's contact patch results in a so-called "aligning torque" about the tire's vertical axis Z. The tire lateral force FY_W acts at the centroid of the surface made up by the shear stress distribution. The distance from this centroid to the tire's lateral axis is called the tire's pneumatic trail. As a result of this offset, the tire lateral force FY_W acts at a point in the contact patch behind the tire's lateral axis Y. In this case, the pneumatic trail acts as a lever arm for the lateral force and causes a moment MZ_W which tends to reduce the sideslip angle of the wheel, thereby returning the vehicle to straightline driving. Figures depicts a family of curves for the aligning moment MZ,W as a function of the tire sideslip angle α. As can be seen the curves of the aligning torque show a pronounced maximum at a sideslip angle of α = 3° to 6°. A further increase in the lateral force FY_W cannot compensate for the decreased pneumatic trail. Thus, at large values of the sideslip angle α, the aligning moment can switch signs and become negative, which causes the wheels to turn further.

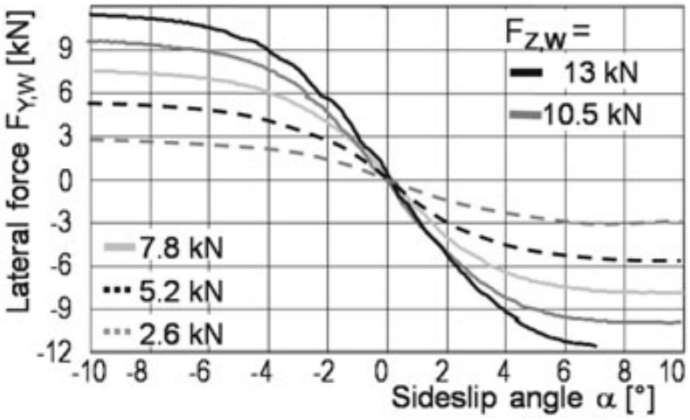

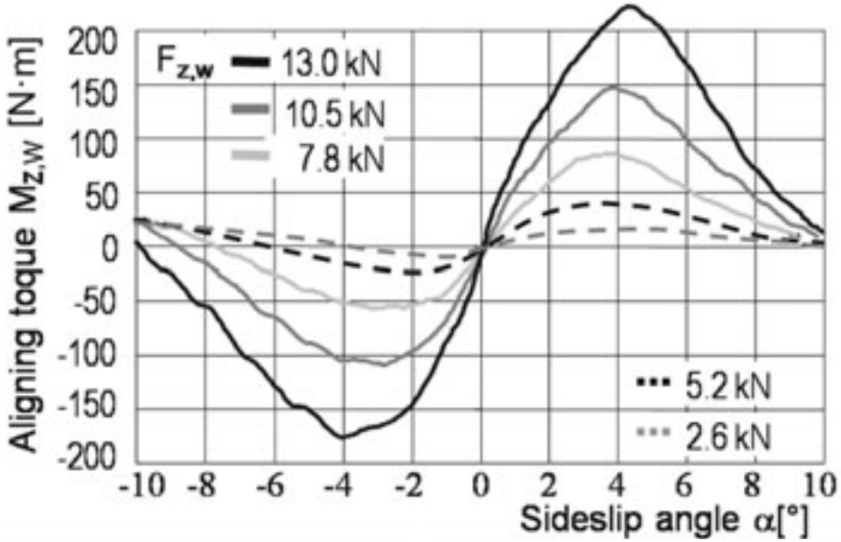

*Chassis Handbook, M. ERSOY, B. Heissing

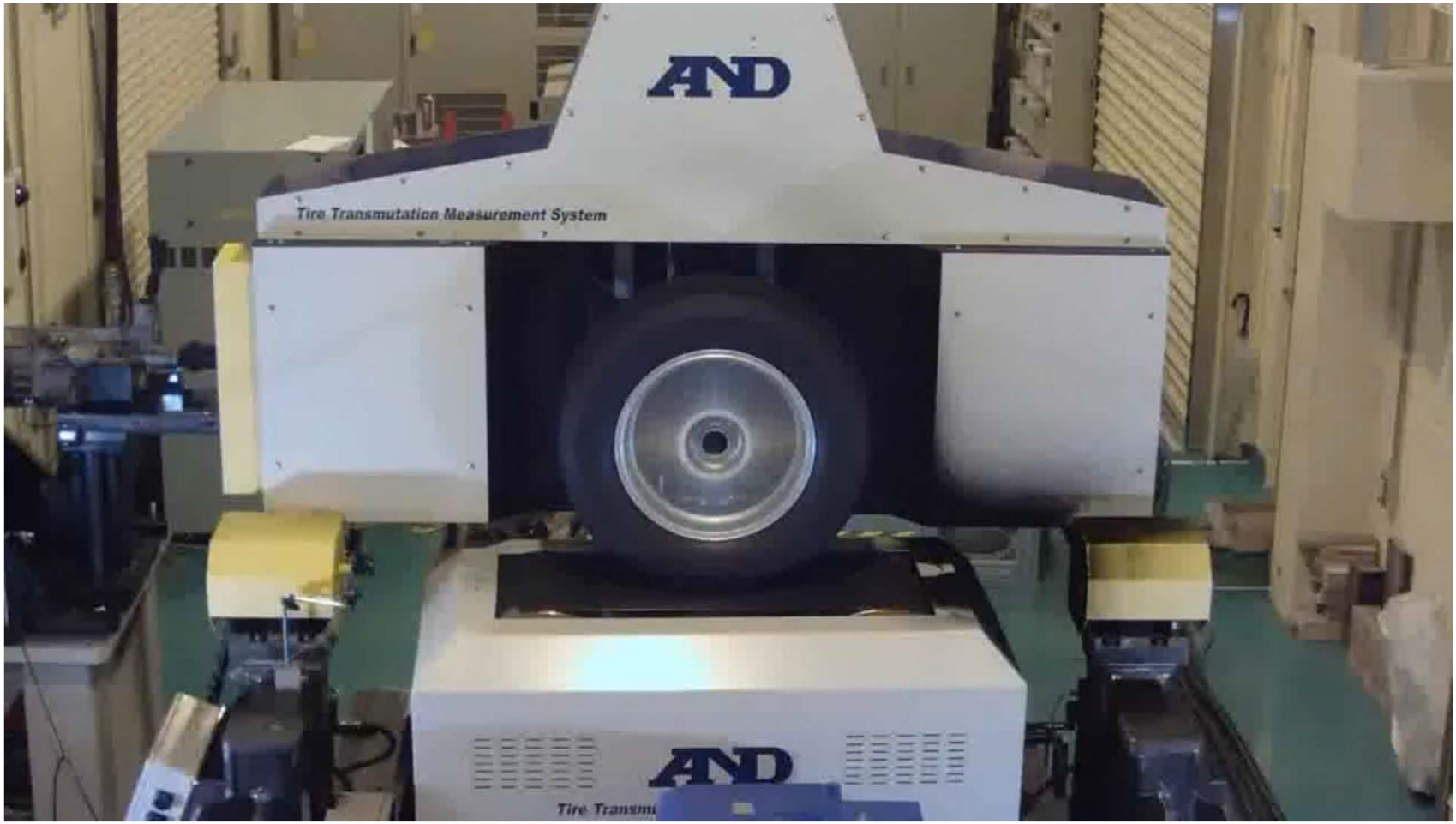
AND
Tire Transmutation Measurement System
AND